

UNIVERSITÀ DEGLI STUDI DI BOLOGNA

FACOLTA' DI MEDICINA E CHIRURGIA

Dottorato di Ricerca in Scienze Pneumo-Cardio-Toraciche
di interesse Medico e Chirurgico

**PRE-CLINICAL IMAGING: SMALL ANIMAL PET AND CT
APPLICATIONS IN PNEUMOLOGY, ONCOLOGY AND
CARDIOLOGY**

**Tesi di Dottorato di Ricerca in Scienze Pneumo-Cardio-Toraciche
di interesse Medico e Chirurgico**

Coordinatore del Dottorato

Prof Sandro Mattioli

Relatore

Prof Sandro Mattioli

Presentata da

Dott.ssa Valentina Ambrosini

Settore Scientifico-Disciplinare: MED36

“The best designers in the world all squint when they look at something. They squint to see the forest from the trees — to find the right balance. Squint at the world. You will see more, by seeing less”.

*John Maeda
Associate Director of Research, Media Arts and Sciences,
Massachusetts Institute of Technology*



ALMA MATER STUDIORUM-UNIVERSITÀ DI BOLOGNA
DIPARTIMENTO DI DISCIPLINE CHIRURGICHE, RIANIMATORIE E DEI TRAPIANTI
DOTTORATO DI RICERCA IN
SCIENZE MEDICHE SPECILISTICHE
PROGETTO: "SCIENZE PNEUMO-CARDIO-TORACICHE DI INTERESSE MEDICO E
CHIRURGICO"

Policlinico S. Orsola - Malpighi - Via Massarenti, 9 - 40138 Bologna (ITALY)
Tel. e fax 0039 051.347431 Email sandro.mattioli @ unibo.it

OMISSIS

Dott. ssa Valentina Ambrosini

Curriculum Seguito Indirizzo Internistico – Malattie dell'Apparato Respiratorio

Titolo tesi di Dottorato "PRE-CLINICAL IMAGING: SMALL ANIMAL PET AND CT APPLICATIONS IN PNEUMOLOGY, ONCOLOGY AND CARDIOLOGY".

Presentazione La Dott.ssa Ambrosini ha prevalentemente sviluppato studi sulle applicazioni cliniche e pre-cliniche della PET in oncologia, pneumologia e cardiologia. L'attività di ricerca pre-clinica è stata focalizzata allo studio, mediante PET per piccoli animali, di modelli murini di neoplasia umana (carcinoma del polmone e linfoma) e di modelli di infarto miocardico indotto chirurgicamente in ratti.

L'attività di ricerca, clinica e pre-clinica, è stato eseguita presso il **Dipartimento di Scienze Radiologiche ed Istocitopatologiche dell'Università' di Bologna**, sotto la supervisione del **Prof Mario Fabbri**, svolgendo attività presso il **Laboratorio di Imaging Pre-clinico** ed il **Centro PET della UO di Medicina Nucleare del Policlinico S.Orsola-Malpighi, Bologna**.

I **risultati preliminari** suggeriscono che la PET è una tecnica molto utile per selezionare gli animali in cui la neoplasia ha attecchito, per monitorare la crescita tumorale nel tempo, fornendo utili indicazioni sull'attività metabolica delle lesioni. La PET per piccoli animali è inoltre utile per la valutazione dell'estensione dell'area infartuale indotta chirurgicamente nell'animale e può essere utilizzata per valutare il recupero funzionale del miocardio dopo terapie rigenerative sperimentali



ALMA MATER STUDIORUM-UNIVERSITÀ DI BOLOGNA
DIPARTIMENTO DI DISCIPLINE CHIRURGICHE, RIANIMATORIE E DEI TRAPIANTI
DOTTORATO DI RICERCA IN
SCIENZE MEDICHE SPECILISTICHE
PROGETTO: "SCIENZE PNEUMO-CARDIO-TORACICHE DI INTERESSE MEDICO E
CHIRURGICO"

Policlinico S. Orsola - Malpighi - Via Massarenti, 9 - 40138 Bologna (ITALY)
Tel. e fax 0039 051.347431 Email sandro.mattioli @ unibo.it

La Dott.ssa Ambrosini ha svolto la sua attività di ricerca con dedizione e profitto degni di nota.

Il suo lavoro, documentato dalle pubblicazioni prodotte, è stato apprezzato ed è valutato come eccellente dal Collegio dei Docenti del Dottorato.

Il Coordinatore

Prof. Sandro Mattioli

INDEX

1. Section 1: Introduction to pre-clinical imaging page 6

2. Section 2: Small animal PET and CT applications in Pneumology (murine model of lung squamous cells carcinoma) page 10

3. Section 3: Small animal PET applications in Oncology (murine xenograft model of anaplastic large cells human lymphoma) page 22

4. Section 4: Small animal PET applications in Cardiology (rat model of hear infarction) page 34

5. Conclusions page 45

SECTION 1

INTRODUCTION TO PRE-CLINICAL IMAGING

Pre-clinical imaging may be defined as ‘the visual representation, characterization, and quantification of biological processes at the cellular and sub-cellular levels within intact living organisms. It is a novel multidisciplinary field, in which the images produced reflect cellular and molecular pathways and in-vivo mechanisms of disease present within the context of physiologically authentic environments’ [1].

Conventional imaging technologies rely mostly on non-specific morphologic changes to differentiate pathologic from normal tissues rather than identifying specific molecular events responsible for the presence of disease. On the contrary, molecular imaging exploits specific molecular probes as the source of image contrast. Imaging is a novel approach to early detect the presence of disease (e.g. early diagnosis of tumour) and to monitor the metabolic changes over time. Moreover, novel strategies , such as the reporter-gene/reporter-probe, allow the in-vivo detection of gene-expression.

The advent of molecular imaging strategies follows the recent advances in molecular and cell biology techniques, the use of transgenic animal models, the availability of newer imaging drugs and probes that are highly specific, and the development of high resolution small-animal imaging instrumentation.

Molecular imaging in living subjects offers distinct advantages when compared with conventional in vitro and cell culture research and it can be considered as a bridge between in-vitro studies and clinical practice. The main advantages of molecular imaging can be summarized as follows: it eliminates the need to kill mice as part of their phenotype determination; by serial imaging of the same animal over time, it is possible to acquire functional data of disease progression and allows to identify mutants that are otherwise difficult to interpret with data taken at a single time point; it allows concomitant visual and analytical biological phenotyping of animals; and it offers the researcher the opportunity to study the disease using multiple imaging strategies (e.g., by using different imaging reporter probes or modalities). Basically all imaging modalities used in humans can be employed in rodent models (PET, CT, MRI, US, optical imaging, SPECT) of disease (Figure 1.1).

Small animal PET (Positron emission tomography) and CT (computed tomography) are the imaging modalities used in the protocols described in this thesis work.

The first author to suggest small animal PET as a ‘sensitive and informative tool to study biological processes’ was Michael Phelps in 2000 [2]. Small animal PET offers several

advantages for animal studies. It is a whole-body, functional, non-invasive technique that allows repetitive imaging of the same animal over time, therefore reducing the total number of animals used for each experiment and offering the advantage of closely following the metabolic changes of the disease under study in the same animal at different time-points. For this reason, small animal PET is a promising tool to assess the response to novel drugs and to evaluate the bio-distribution of novel PET tracers. Another relevant advantage of small animal PET is the very high spatial resolution (approximately 1,2-1,6mm). Recently it was also used to in-vivo assess gene expression using the reporter-gene/reporter probe approach.

Positron emission tomography records high-energy X-rays emitted from within the subject. Natural biological molecules can be labelled with a positron-emitting isotope that is capable of producing two X-rays through emission of a positron from its nucleus, which eventually annihilates with a nearby electron to produce two 511,000-eV X-rays at $\approx 180^\circ$ apart. Positron-emitting isotopes frequently used include ^{15}O , ^{13}N , ^{11}C , and ^{18}F , the latter used as a substitute for hydrogen. Other less commonly used positron emitters include ^{14}O , ^{64}Cu , ^{62}Cu , ^{124}I , ^{76}Br , ^{82}Rb , and ^{68}Ga . Most of these isotopes are produced in a cyclotron [3], but some can be produced using a generator (e.g., ^{68}Ga , ^{82}Rb). Labelled molecular probes or tracers can be introduced into the subject intravenously and PET imaging can be performed in the anaesthetized animal. Data on the distribution and concentration of the radiotracer can be acquired. The most commonly used tracer in animal studies, as well as in humans, is ^{18}F -FDG, a glucose analogue labelled with ^{18}F that is avidly taken up by highly proliferating cells (such as inflammatory cells or tumour cells) and is trapped inside the cell by phosphorylation. Other radiotracers currently available include ^{11}C -Choline, ^{11}C -Methionine, ^{68}Ga -DOTANOC and ^{18}F -DOPA.

The sensitivity of PET is relatively high in the range of 10^{-11} – 10^{-12} mole/L, and is independent of the location depth of the reporter probe of interest. Typically, several million cells accumulating reporter probe have to be in relative close proximity for a PET scanner to record them as a distinct entity relative to the background [1].

The accuracy of small animal PET functional data can be increased using an anatomic imaging modality that allows a better localization of high radiotracer uptake areas. Images in computed tomography are obtained when component tissues differentially absorb X-rays as they pass through the body [4]. A low-energy X-ray source of 30–50 kVp (of considerably lower energy than in clinical CT scanners) and a detector rotate around the animal, acquiring volumetric data. Most mouse CT images are collected with high-resolution phosphor screen/CCD detectors to optimize image quality. A scan of an entire mouse at 100- μm

resolution takes \approx 15 min. Higher-resolution (50- μ m) images are achievable with longer scanning times (that however imply a higher dose delivered). The system spatial resolution is primarily limited by the pixel sampling rate, the X-ray source size, and blurring in the phosphor screen. A limit of performing CT in living animals is the radiation dose (0.6 Gy per scan; 5% of the LD50 for mice), that can limit serial imaging of the same animal over time. Unlike MRI, CT has relatively poor soft tissue contrast, often making it necessary to administer iodinated contrast media to delineate organs or tumours. Dedicated high-resolution small animal CT scanners are currently available for anatomical imaging of animal models of disease [5,6,7], thus complementing the functional information obtained by other modalities.

Aim of this thesis work was to assess the usefulness of small animal PET and CT in the assessment of different rodent models of human disease (squamous cells lung carcinoma, anaplastic large cells lymphoma and ischemic heart disease).

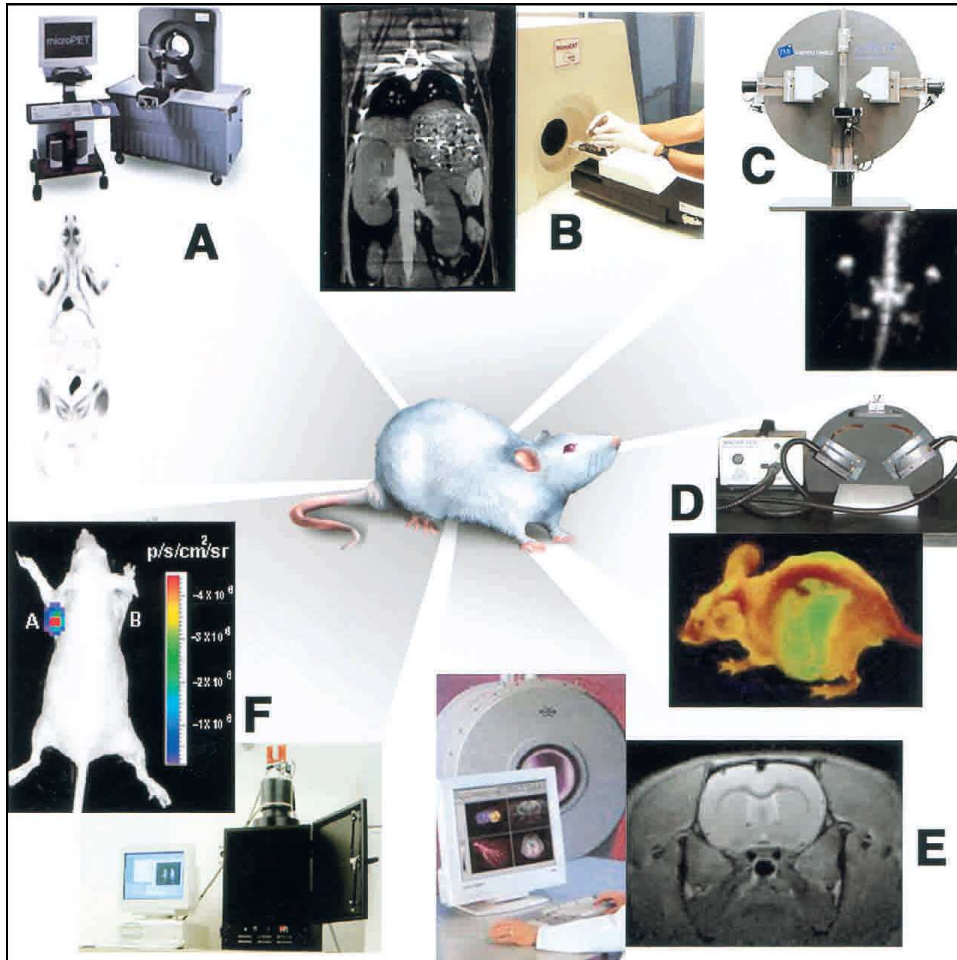
REFERENCES SECTION 1

1. Massoud TF, Gambhir SS. Molecular imaging in living subjects: seeing fundamental biological processes in a new light. *Genes Dev.* 2003 Mar 1;17(5):545-80.
2. Phelps ME. Inaugural article: positron emission tomography provides molecular imaging of biological processes. *Proc Natl Acad Sci U S A.* 2000 Aug 1;97(16):9226-33.
3. Strijckmans 2001 Strijckmans, K. 2001. The isochronous cyclotron: Principles and recent developments. *Comput. Med. Imaging Graph.* 25: 69–78.
4. Dendy, P. and Heaton, B. 1999. Tomographic imaging. In *Physics for diagnostic radiology* (eds. P. Dendy and B. Heaton), pp. 249–278. Institute of Physics, Bristol, UK.
5. Paulus, M.J., Gleason, S.S., Easterly, M.E., and Foltz, C.J. A review of high-resolution X-ray computed tomography and other imaging modalities for small animal research. *Lab. Anim. (NY)* 2001: 30: 36–45.
6. Berger, F., Lee, Y.-P., Loening, A.M., Chatziioannou, A., Freedland, S.J., Leahy, R., Lieberman, J.R., Belldegrun, A.S., Sawyers, C.L., and Gambhir, S.S. Whole-body skeletal imaging in mice utilizing microPET: Optimization of reproducibility reproducibility and applications in animal models of bone disease. *Eur. J. Nucl. Med. Mol. Imaging* 2002: 29: 1225–1236.;
7. Holdsworth, D.W. and Thornton, M.M. Micro-CT in small animal and specimen imaging. *Trends Biotechnol.* 2002: 20: S34–S39.)

FIGURES SECTION 1

Figure 1.1 Multiple imaging modalities are available for small-animal molecular imaging. (A) microPET, (B) microCT, (C) microSPECT, (D) Optical reflectance fluorescence, (E) microMRI, (F) Optical bioluminescence.

Massoud TF, Gambhir SS. Genes Dev. 2003 Mar 1;17(5):545-80.



SECTION 2

SMALL ANIMAL PET and CT APPLICATIONS IN PNEUMOLOGY (murine model of lung squamous cells carcinoma)

ABSTRACT

Background: small animal imaging has become a relevant research field in pre-clinical oncology. In particular, metabolic information provided by small animal PET are very useful to closely monitor tumour growth and assess therapy response in murine models of human disease. Although there are various murine models for human lung adenocarcinomas, models for squamous cells lung carcinoma, the most frequent form of human cancer, are few.

Aim: to assess the feasibility of 18F-FDG small animal PET to monitor tumour growth in a chemically induced model of lung squamous cells carcinoma.

Materials and Methods: 19 NIH Swiss mice were skin painted by NTCU (*N*-nitroso-tris-chloroethylurea) twice a week with a three day interval for 8 months and 10 NIH Swiss mice skin painted with NTCU-solvent (acetone) were used as controls. 18F-FDG PET was performed under sevoflurane anaesthesia and oxygen supplementation at 2,4,6 and 8 months from initial treatment. Images were assessed by visual analysis and semiquantitatively: considering the diffuse distribution of tumour development, the mean of the counts/pixel measured at three lung levels (TLA), corrected for the effective dose injected and for decay, was used for comparison between cases and controls. Pathological evaluation was carried out from the time of the first positive PET results in a subgroup of the whole population to assess correlation with PET findings. Small animal CT was performed at 8 months in an animal subgroup.

Results: In both terms of visual analysis and measure of total lung activity, 18F-FDG PET at 2 and 4 months from initial treatment were comparable in cases and controls. At 6 months, PET images showed a faint and diffuse uptake over both lung fields with multiple focal areas of increase tracer uptake that merged into confluent masses at 8 month, seriously subverting lung architecture. Total lung activity was significantly higher in cases vs controls at 6 ($p=0,00000668$) and 8 months ($p=0,00000043$) from initial treatment and paralleled the progressive lung involvement and histological severity.

Conclusions: 18F-FDG PET may be useful in the assessment of this chemically induced murine model of lung squamous cells carcinoma. The TLA may be used as a measure of

tumour metabolic activity of the tumour-bearing animals and may be useful in new drug testing studies.

INTRODUCTION

Lung cancer is the most common cause of death for cancer in both man and women in developed countries [1]. The role of ¹⁸F-FDG PET in the assessment of lung cancer is well established in humans for the characterization of lung lesions, diagnosis, initial staging, early assessment of tumour response to therapy and early identification of disease relapse [2,3,4,5]. Moreover, PET is a novel technology for molecular imaging essays of gene expression, signal transduction and evaluation of the outcomes of processes being modified in the mouse or in the patient, that offers the advantage of providing in vivo biological characterization of the disease [6]. The recent development of small animal PET scanners represents a new and non invasive approach to study rodent model of human disease, providing a novel tool to closely follow tumour growth over time, to test new anticancer drugs and to study the biological processes at the basis of tumour transformation [7].

Mouse models of tumourigenesis of many human tumours are currently available and are widely used in both basic research and therapeutic trials [8,9,10]. The best murine models of human disease are able to accurately reproduce aspects (angiogenesis, tumour-stromal interaction, hormone dependency) of human cancer development and molecular mechanisms at the basis of tumourigenesis, tumour progression and metastasis, thus representing a useful tool to study human carcinogenesis [8,10].

Murine lung tumours present many similarities with the human counterparts [9] and different murine models of lung carcinogenesis are currently available [11,12,13]. The most commonly used xenograft models [14-20] obtained by subcutaneous or intratracheal injection of human derived tumour cell lines require an immunocompromised host and lack their original microenvironment, including tumour derived stroma that has been recently shown to play a role in tumour development and progression. Although there are well established transgenic models of adenoma and adenocarcinoma [21,22], there is no well established model of squamous cells carcinoma [11]. Since squamous cells carcinoma is by far the most frequent form of lung cancer and drug efficacy may vary among different histotypes, it is crucial to identify a reproducible murine model of squamous cells carcinoma. The first report of squamous cell carcinoma induced in non-immunocompromised mice by NTCU (*N*-nitroso-tris-chloroethylurea) is by Lijinsky et al in 1988 [23]. The same experiment was later repeated by Wang et al [11] who reported how different mouse strains presented variable tumour

susceptibility to NTCU and the NIH Swiss strain presented the highest tumour susceptibility. Moreover, they demonstrated that NTCU-induced tumours presented many similarities with the histopathological features of human squamous cells carcinoma.

The aim of the present study was to assess non small cells lung cancer (NSCLC) development in a chemically-induced (using *N*-nitroso-tris-chloroethylurea, NTCU) mouse model of squamous cells carcinoma of the lung by small animal PET.

MATERIALS AND METHODS

To induce NSCLC development, nineteen 7 weeks old, female NIH Swiss mice were skin painted with a known mutagen (*N*-nitroso-tris-chloroethylurea, NTCU), according to the protocol proposed by Wang [11]. Forty-eight hours after dorsal shaving, each animal was skin painted with a drop of NTCU (0.04M, 25ul) twice a week, with a 3-day interval for 8 months. Ten 7 weeks old, female NIH Swiss mice, were used as controls and were skin painted with the same amount of NTCU solvent (Acetone).

Animals were handled and closely monitored for their health at the IOR-Istituti Ortopedici Rizzoli, Bologna. All experiments were approved by the Ethical Committee of the University of Bologna.

PET scans were carried out under sevoflurane (5%) anaesthesia (VetEquip Complete Anaesthesia System, Pleasanton, CA) and oxygen supplementation (1L/min). Each anaesthetised animal was injected with 20 MBq of ¹⁸F-FDG in the tail vein (injected volume <0,15ml) and subsequently allowed to wake up during the uptake time (60minutes). The residual dose in the syringe was measured to verify the effective dose injected. At the end of the uptake time, PET image acquisition was performed with a small animal PET tomograph (GE eXplore Vista DR) in the anaesthetised mouse placed prone on the scanner bed (2 bed positions, 15minutes/each bed position). Once the scan was completed the animal was allowed to wake up in a warmed recovery box.

¹⁸F-FDG PET was performed at 2, 4, 6 and 8 months from the initial treatment with either NTCU or Acetone. FDG-PET images were reconstructed iteratively (OSEM 2D) and read in three planes (axial, sagittal and coronal). The scan was considered positive if any area of increased non-physiologic FDG uptake was observed.

CT scans were carried out using a small animal CT tomograph (GE eXplore Locus) in two cases and in two controls, at 8 months from initial skin painting (). ¹⁸F-FDG filled microspheres were fixed with adhesive tape on the animal body and used as reference marks to accurately fuse CT and PET separately acquired images.

Pathology sections were obtained from the time of the first positive PET scan in a subgroup of the whole sample. Three cases were sacrificed after the third PET and six animals (four cases and 2 controls) were sacrificed after the fourth PET scan and autopsy was carried out.

Data analysis

Continuous variables were expressed as mean±standard deviation. Differences among groups were considered significant when $p < 0,005$.

Considering the disease diffuse distribution over the lung fields, for PET image analysis the lungs were considered at three axial levels: lung apex, mid-lung and lung bases. For each level, mean counts/pixel were recorded in a region of interest including all lung fields. Total lung activity (TLA) was calculated for each animal as the mean of the three levels. TLA was normalized for the injected dose (TLA_I) in each case and corrected for decay ($TLA_I = TLA / (\text{injected dose} - \text{residual dose})$).

For each PET scan, mean TLA_I was calculated for cases and controls and data were compared using the T-test for unpaired data.

RESULTS

In our study a chemically induced murine model of squamous cells carcinoma was used to in-vivo monitor tumour development over time by small animal PET at 2,4,6, and 8 months from initial treatment. Overall, PET scan was performed in 19 cases and 10 controls at 2 and 4 months from initial treatment, in 15 cases and 9 controls at 6 months, in 5 cases and 9 controls at 8 months.

In our series we observed some mortality after four months from initial treatment (4 cases and 1 control were found dead in their cages between four and six months; 6 cases were found dead at 7 months) and case mice presented a significant ($p < 0,0002$) lower weight than controls (Figure 2.1). It was not possible to perform autopsy in any of these animals. Pathological studies were performed starting from the time of the first PET positive result. Three animals were sacrificed after the third PET scan and four animals and two controls after the fourth PET acquisition.

At 2 and 4 months from initial treatment, both case and control mice showed similar findings at ^{18}F -FDG PET. Starting from the third scan (6months), it was possible to detect the presence of a diffuse lung disease with a faint background FDG uptake with multiple areas of increased tracer uptake in NTCU-treated mice. FDG-positive areas merged into confluent

areas of pathological uptake involving all lung fields in the images acquired at 8 months from initial treatment (Figure 2.2).

To quantify the activity in the whole lung, the mean of the activity measured at three lung levels (TLA_I) was used for comparison between cases and controls. There were no differences in FDG uptake in the two groups in the earliest scans while in the latest PET acquisitions the tracer uptake was significantly higher in mice treated with NTCU (Figure 2.3). In particular, mice skin-painted with NTCU showed the highest values (PET at 6 months: $TLA_{Icases}=39.5$ vs $TLA_{Icontrols}=20.3$, $p=0,00000668$; PET at 8 months: $TLA_{Icases}=48.8$ vs 25.6 , $p=0,00000043$).

Mean TLA_I increase in case mice over time reflects the progressive changes observed in the histological sections obtained from the first PET positivity in a subgroup of the whole sample. Overall, histological evaluation was carried out in nine animals (3 cases after the third PET scan, 4 cases and 2 controls after the fourth PET scan). Pathologic evaluation of the lungs of the three cases sacrificed at 6 months, when TLA_I was double the one observed in controls, demonstrated the presence of diffuse inflammation involving all lung fields with lymphocytes inflammatory exudate filling the alveoli, foci of bronchial epithelial hyperplasia and metaplasia and multiple nests of squamous cells carcinoma with a prominent central distribution (Figure 2.4A-B). Among the animals sacrificed after the fourth scan, control animals had normal lung fields and intact lung architecture (Figure 2.4C) while in the NTCU-treated mice lung architecture was completely subverted, with squamous tumour cells infiltrating the air spaces and franc bronchiolar epithelium metaplasia and displasia (Figure 2.4D-E). Squamous cells carcinoma areas appeared as non-capsulated masses, with stratified squamous cells with hyperchromatic nuclei, irregularly shaped and forming sheet or nests of tumour cells all over the lungs.

Comparing the trend of TLA over time in the animals in which 4 PET scans were performed and histological evaluation after 8 months from initial treatment was available, mean TLA_{Icases} was significantly higher than $TLA_{Icontrols}$ starting from the third acquisition.

Small animal CT performed at the end of the fourth PET scan in two cases showed the presence of increased attenuation involving all lung fields and with solid confluent nodules corresponding on fused images at the areas of increased FDG uptake.

DISCUSSION

PET is widely used in human oncology and its role in the assessment of lung tumour bearing patients is well documented. Since lung cancer is still the leading cause of tumour death in western countries, it is crucial to identify animal models that accurately reproduce the features

of the human disease, in order to have a valid tool to study both the mechanisms at the basis of carcinogenesis and to test potentially therapeutic new drugs.

Recent advances in in-vivo animal imaging offer many advantages for studying animal models of human disease over conventional in vitro studies [24,25,26]. In particular, small animal PET is an in-vivo whole body, non-invasive technique that allows repetitive imaging of the same animal over time, providing information on the metabolic activity of the pathologic areas, allowing to closely monitor tumour growth and avoiding the need to sacrifice the animal at fixed time intervals [7,24]. Moreover, animal PET studies have a high spatial resolution and allow both a visual analysis of the pathologic areas and a numerical measure of the biological phenomena under study [27]. This is particularly helpful in drugs efficacy studies, where the reduction in lesion size alone is an inaccurate measure of drug response, while the possibility to compare the lesions metabolic activity before and after the drug administration directly reflects the changes in the tumour viable cell fraction.

Murine models of lung squamous cells carcinoma were reported to accurately reproduce the human tumour features. The induction of squamous cells carcinoma by NTCU was first described in 1988 [23] and the experiment was recently repeated in different strains of mice to test their susceptibility to tumour development [11].

In this paper, we repeatedly studied a group of 19 NTCU-treated mice by ¹⁸F-FDG small animal PET (every 2 months, up to 8 months) and used 10 mice treated with NTCU solvent as controls.

Our data show that although the results of the first two PET acquisitions were comparable in cases and controls in terms of both visual analysis and measure of lung activity, significant changes were observed starting from the third PET acquisition, when pathology sections revealed the presence of sparse nests of squamous cancer cells, bronchial metaplasia and alveoli-filling inflammatory exudate in NTCU-treated mice. At 6 months NTCU-treated mice presented multiple areas of increased FDG uptake on a diffusely faint uptake background while in the images acquired at 8 months FDG-positive areas merged into masses that involved almost all lung fields. To semiquantify the total activity present in the tumour-bearing lungs, we used a metabolic parameter (TLA) derived from the mean activity at three lung levels. The TLA increased over time only in case mice starting from the third PET acquisition and further increased at the fourth PET scan, while remained always low in controls. Although this murine model has been well documented from an histological point of view (<http://emice.nci.nih.gov>), pathological studies were performed starting from the time of

the first PET positive result to assess if TLA could be used to non-invasively monitor tumour bearing animals.

At the time of the first PET positive result, when pathology confirmed the presence of multiple areas of tumour cells arranged in either nests or with a lobular distribution that effaced the normal pulmonary architecture, NTCU-treated mice presented a TLA double the one observed in controls. TLA further increased at 8 months, when PET images showed an even more diffused disease and pathology revealed large areas of neoplastic cells with almost no spared lung parenchyma.

TLA correlated well with disease presence and with the progressive changes observed on histological sections, revealing the presence of disease from 6 months from initial treatment and an increased tumour burden and a more aggressive disease in the latest scans.

Ideally, the effect of new anticancer drugs should be assessed on the early phases of tumour development, to ensure the presence of small well-vascularized nodules with highly proliferating cells and with no necrotic areas. Small animal PET may be used in new drugs testing studies to identify tumour-bearing animals in early phases of cancer development, and our data show that in this murine model changes in TLA closely reflect the progressive changes from multiple areas of tumour cells and metaplasia to widespread tumour. Since we observed an increase in TLA with increasing tumour burden, the measure of TLA might be useful in studies assessing the efficacy of new anticancer drugs in this murine model.

Small animal CT performed at 8 months after the fourth PET confirmed the diffuse pattern of disease distribution and showed that increased attenuation areas identified by CT corresponded to increased FDG uptake areas in PET images.

It is to be noted that although the NIH Swiss mice were reported to be the most resistant to NTCU-induced toxicity among eight different mouse strains [11], we observed some mortality starting from four months after initial treatment, with our initial population reducing of 40% at the end of the experiment. Unfortunately we could not perform autopsy in the mice that we found dead in their cages. Since there were no signs of any infectious disease in the other mice kept in the same cages of the ones who died, we can speculate their deaths were only related to NTCU-induced toxicity. It would be interesting to know if lower NTCU-doses for a shorter period of time would invariably lead to tumour formation and to lower toxicity and in this contest small animal PET studies may be useful in the early assessment of tumour development.

In preclinical studies it is crucial to identify the most suitable animal model for the disease or the biological process under study. The present murine model of human squamous cells

carcinoma offers the advantage of accurately reproducing the features of the human tumour, recapitulating all the steps from epithelial hyperplasia to carcinoma and our data show that it is possible to closely monitor disease progression by measuring total lung activity in serial PET scanning. In particular, ¹⁸F-FDG small Animal PET can identify tumour formation as early as 6 months from initial treatment. Nevertheless the high mortality we experienced may rise the question of whether it would be possible to induce tumour formation with lower NTCU doses to reduce toxicity.

FUTURE DIRECTIONS..

Although this model is quite accurate in reproducing the pathological steps of human tumour development, it takes a long time to induce tumour formation and the diffuse nature of lung involvement renders semi-quantitative analyses of tumour activity more difficult (ideal condition would be a high uptake area over a cold background), therefore in the next future murine xenograft models of human lung cancer will be studied by small animal PET in order to assess if they can represent more suitable models for tumour assessment and for drug testing studies.

REFERENCES SECTION 2

1. Spiro SG, Silvestri GA. One hundred years of lung cancer. *Am J Respir Crit Care Med.* 2005 Sep 1;172(5):523-9.
2. Higashi K, Matsunari I, Ueda Y, Ikeda R, Guo J, Oguchi M, Tonami H, Yamamoto I. Value of whole-body FDG PET in management of lung cancer. *Ann Nucl Med.* 2003 Feb;17(1):1-14.
3. Vansteenkiste J, Fischer BM, Doooms C, Mortensen J. Positron-emission tomography in prognostic and therapeutic assessment of lung cancer: systematic review. *Lancet Oncol.* 2004 Sep;5(9):531-40.
4. Bunyaviroch T, Coleman RE. PET evaluation of lung cancer. *J Nucl Med.* 2006 Mar;47(3):451-69.
5. Spiro SG, Porter JC. Lung cancer--where are we today? Current advances in staging and nonsurgical treatment. *Am J Respir Crit Care Med.* 2002 Nov 1;166(9):1166-96.
6. Phelps ME. PET: the merging of biology and imaging into molecular imaging. *J Nucl Med.* 2000 Apr;41(4):661-81.4.
7. Herschman HR. Micro-PET imaging and small animal models of disease. *Curr Opin Immunol.* 2003 Aug; 15(4):378-84.

8. Lyons SK. Advances in imaging mouse tumour models in vivo. *J Pathol*. 2005 Jan;205(2):194-205.
9. Malkinson AM. Primary lung tumors in mice as an aid for understanding, preventing, and treating human adenocarcinoma of the lung. *Lung Cancer*. 2001 Jun; 32 (3) :265-79.
10. Maddison K, Clarke AR. New approaches for modelling cancer mechanisms in the mouse. *J Pathol*. 2005 Jan;205(2):181-93.
11. Wang Y, Zhang Z, Yan Y, Lemon WJ, LaRegina M, Morrison C, Lubet R, You M. A chemically induced model for squamous cell carcinoma of the lung in mice: histopathology and strain susceptibility. *Cancer Res*. 2004 Mar 1;64 (5):1647-54.
12. Johnson L, Mercer K, Greenbaum D, Bronson RT, Crowley D, Tuveson DA, Jacks T. Somatic activation of the K-ras oncogene causes early onset lung cancer in mice. *Nature*. 2001 Apr 26;410(6832):1111-6.
13. Fisher GH, Wellen SL, Klimstra D, Lenczowski JM, Tichelaar JW, Lizak MJ, Whitsett JA, Koretsky A, Varmus HE. Induction and apoptotic regression of lung adenocarcinomas by regulation of a K-Ras transgene in the presence and absence of tumor suppressor genes. *Genes Dev*. 2001 Dec 15;15(24):3249-62.
14. McLemore TL, Liu MC, Blacker PC et al. Novel intrapulmonary model for orthotopic propagation of human lung cancers in athymic nude mice. *Cancer Res* 1987; 47: 5132–40.
15. McLemore TL, Eggleston JC, Shoemaker RH, et al. Comparison of intrapulmonary, percutaneous intrathoracic intrathoracic and subcutaneous models for the propagation of human pulmonary and nonpulmonary cancer cell lines in athymic nude mice. *Cancer Res* 1988;48:2880–6. *Res* 2000; 6: 297–304.
16. Doki Y, Murakami K, Yamaura T, Sugiyama S, Misaki T, Saiki I. Mediastinal lymph node metastasis model by orthotopic intrapulmonary implantation of Lewis lung carcinoma cells in mice. *Br J Cancer* 1999; 79:1121–6.
17. Wang HY, Ross HM, Ng B, Burt ME. Establishment of an experimental intrapulmonary tumor nodule model. *Ann Thorac Surg* 1997; 64: 216–19. Miyoshi T, Kondo K, Ishikura H, Kinoshita H, Matsumori Y, Monden Y.
18. Onn A, Isobe T, Itasaka S et al. Development of an orthotopic model to study the biology and therapy of primary human lung cancer in nude mice. *Clin Cancer Res* 2003; 9: 5532–9.
19. Miyoshi T, Kondo K, Ishikura H, Kinoshita H, Matsumori Y, Monden Y. SCID mouse lymphogenous metastatic model of human lung cancer constructed using orthotopic inoculation of cancer cells. *Anticancer Res*. 2000 Jan-Feb;20(1A):161-3.

20. Cutz JC, Guan J, Bayani J, Yoshimoto M, Xue H, Sutcliffe M, English J, Flint J, LeRiche J, Yee J, Squire JA, Gout PW, Lam S, Wang YZ. Establishment in severe combined immunodeficiency mice of subrenal capsule xenografts and transplantable tumor lines from a variety of primary human lung cancers: potential models for studying tumor progression-related changes. *Clin Cancer Res.* 2006 Jul 1;12(13):4043-54.
21. Jackson EL, Willis N, Mercer K, Bronson RT, Crowley D, Montoya R, Jacks T, Tuveson DA. Analysis of lung tumor initiation and progression using conditional expression of oncogenic K-ras. *Genes Dev.* 2001 Dec 15;15(24):3243-8.
22. Fisher GH, Wellen SL, Klimstra D, Lenczowski JM, Tichelaar JW, Lizak MJ, Whitsett JA, Koretsky A, Varmus HE. Induction and apoptotic regression of lung adenocarcinomas by regulation of a K-Ras transgene in the presence and absence of tumor suppressor genes. *Genes Dev.* 2001 Dec 15;15(24):3249-62.
23. Lijinsky, W., and Reuber, M. D. Neoplasms of the skin and other organs observed in Swiss mice treated with nitrosoalkylureas. *J. Cancer Res. Clin. Oncol.*, 114: 245–249, 1988.
24. Massoud TF, Gambhir SS. Molecular imaging in living subjects: seeing fundamental biological processes in a new light. *Genes Dev.* 2003 Mar 1;17(5):545-80.
25. Blasberg RG. Molecular imaging and cancer. *Mol Cancer Ther.* 2003 Mar;2(3):335-43.
26. Schuster DP, Kovacs A, Garbow J, Piwnica-Worms D. Recent advances in imaging the lungs of intact small animals. *Am J Respir Cell Mol Biol.* 2004 Feb;30(2):129-38.
27. Phelps ME. Inaugural article: positron emission tomography provides molecular imaging of biological processes. *Proc Natl Acad Sci U S A.* 2000 Aug 1;97(16):9226-33.

FIGURES SECTION 2

Figure 2.1. Variations of body weight in case and controls mice over time. NTCU-treated mice presented a significant weight loss compared with controls.

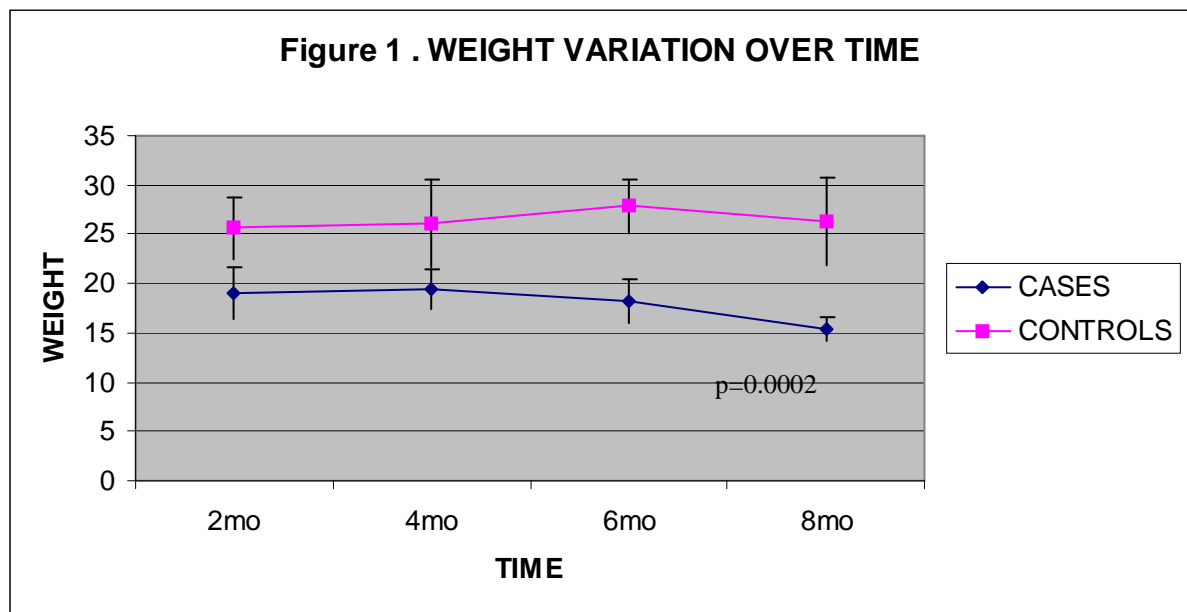


Figure 2.2. ^{18}F -FDG small animal PET and CT axial images of a NTCU-treated mouse at 8 months from initial treatment. ^{18}F -FDG PET showed a diffuse faint background uptake all over the lung fields with multiple areas of focal increased tracer uptake. Positive PET areas corresponded to increased attenuation on CT.

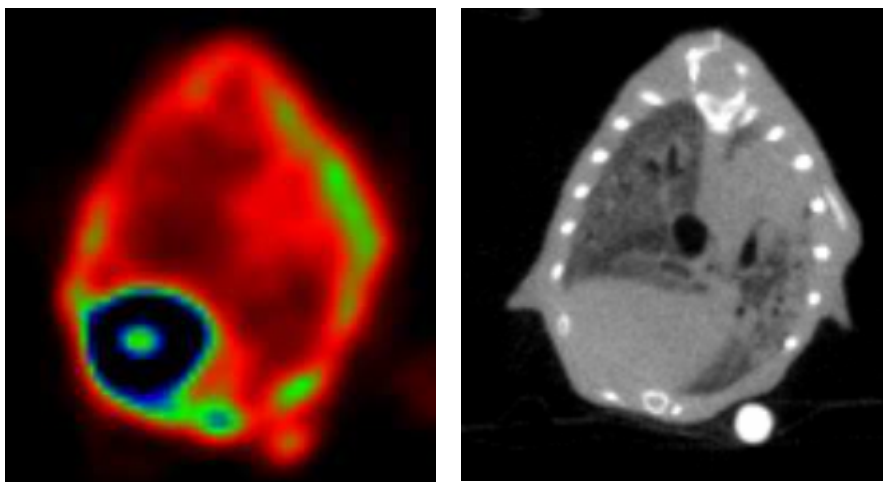


Figure 2.3. Mean TLA variations over time in case and controls mice. Case mice presented a significant TLA increase at the third PET (p=0,00000668) and further more at the fourth PET (p=0,00000043) scan.

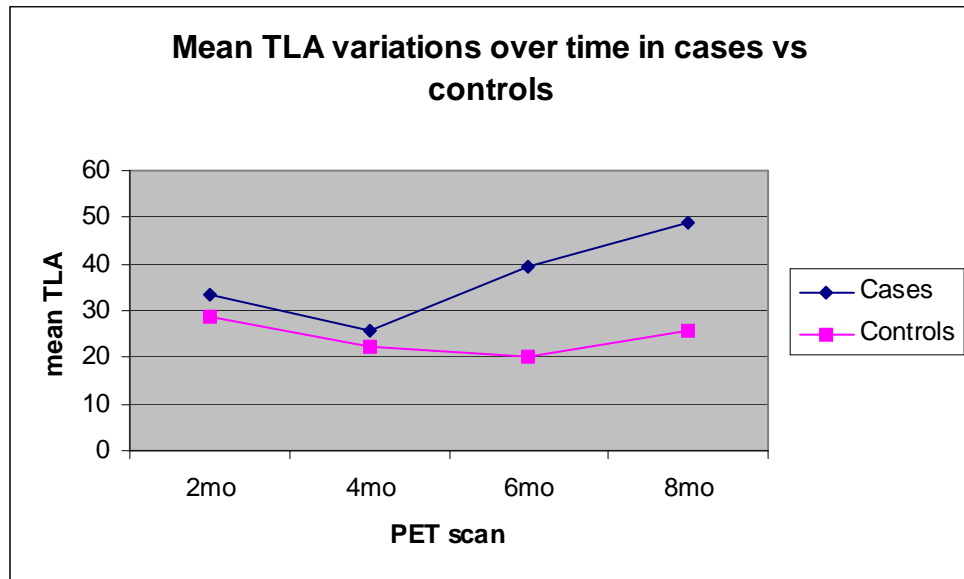
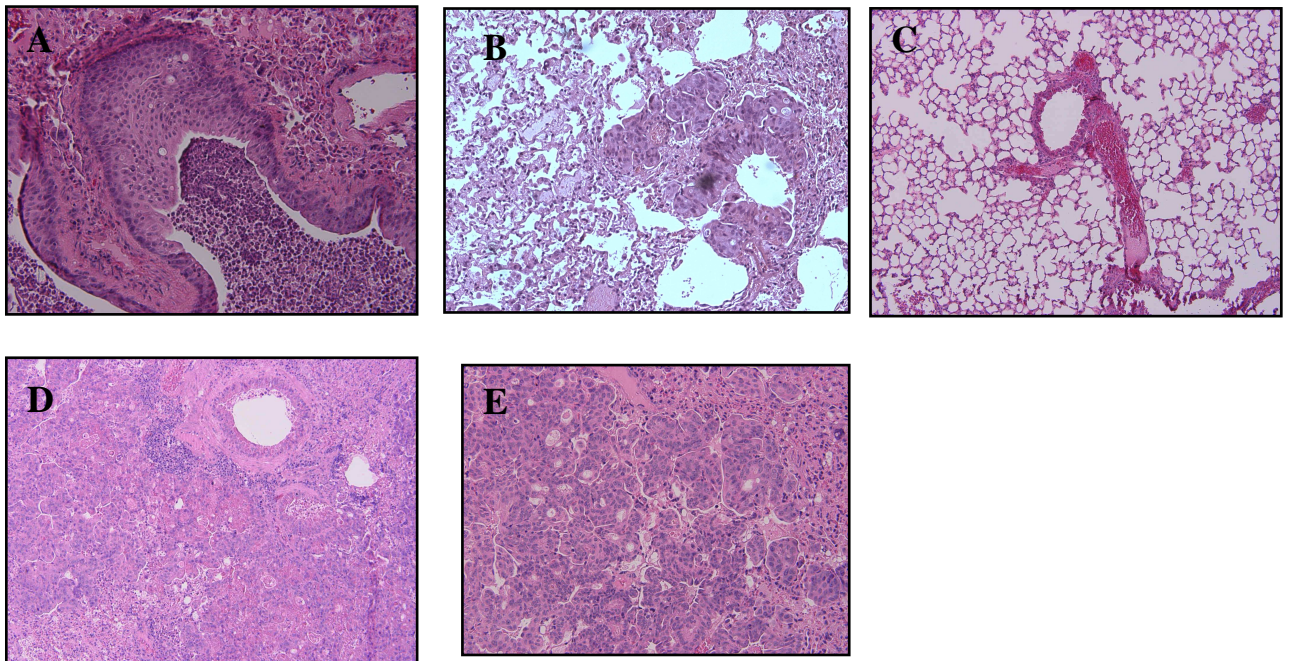


Figure 2.4.



Histological sections of case and control mice. NTCU-treated mouse at 6 months (A, 20x) from initial treatment shows bronchial hyperplasia, inflammatory exudates filling the alveoli and focal areas of squamous cells carcinoma (B, 10x). Normal lung architecture in a control mouse at 8 months (C, 10x). NTCU-treated mouse at 8 months from initial treatment shows a multiple nests of tumour cells infiltrating all lung fields (D, 10x; E, 20x).

SECTION 3

SMALL ANIMAL PET APPLICATIONS IN ONCOLOGY (murine xenograft model of anaplastic large cells human lymphoma)

ABSTRACT

Purpose: to assess if small animal PET is useful to serially monitor the development of a human anaplastic large cells lymphoma (ALCL) murine xenograft and to early select tumour bearing animals.

Methods: Human ALCL Karpas 299 cell line was subcutaneously injected in 6 weeks-old NOD/SCID mice (10^7 cells/mice in 150 uL FBS) at right flank level. Small animal ^{18}F -FDG PET was serially performed (i.v. injected dose: 20MBq in <0.15ml, uptake time: 60 minutes, image acquisition: 1 bed position of 15 minutes): early PET at 2 days after cells inoculation in 4/8 mice and at 4 days in 4/8; later PET scans were performed in all animals at 7, 14, 21, 28 days after inoculation. Images were evaluated visually and the tumour to background ratio (TBR) was used for semi-quantitative analysis. Pathology sections were obtained in all cases.

Results: PET detected the presence of the tumour as early as seven days after inoculation in 4/8 mice and at 14 days in 2/8. Of the two remaining mice, one died after the first PET scan (thus preventing any evaluation of detection time) while the other showed a microscopic neoplastic infiltration at tracheal level at autopsy.

Mean TBR progressively increased in all positive cases, particularly in the first 3 weeks, reaching a plateau afterwards.

Conclusions: PET was positive in 6/8 (75%) animals, detecting the presence of viable tumour cells earlier than macroscopic evaluation, thus may be used to early identify tumour bearing animals.

INTRODUCTION

Primary systemic anaplastic large cells lymphoma (ALCL) accounts for about 5% of all non-Hodgkin lymphomas in adults and 20-30% of large-cell lymphomas in children [1]. ALCL represents a heterogeneous group of aggressive non-Hodgkin lymphomas characterized by strong expression of CD30 and frequent t(2;5) chromosome translocation [2]. Notwithstanding its responsiveness to chemotherapy, about 30-40% of the patients die after intensive treatment and standard therapy is associated with considerable toxicity, particularly bothersome in the paediatric population. Therefore alternative new drugs need to be developed not only for relapsing patients but also as first line treatment.

¹⁸F-FDG PET is widely used for the assessment of lymphoma in human patients for either staging, assessment of the response to therapy and early detection of relapse, influencing in many cases the patients clinical management [3-11].

Presenting many similarities with human disease, murine models of lymphoma are useful tools for pre-clinical studies. In recent years molecular imaging procedures (PET, CT, optical imaging, MRI) have been more and more employed in oncological preclinical studies [12-21]. Among the different imaging techniques, small animal PET shows a good spatial resolution (1.0-1.5 mm) [22] and is the only method allowing sequential evaluation of the same animal over time. Therefore small animal PET is particularly useful for monitoring the metabolic features of a lesion, representing a valid tool to assess the response to treatment [23]. The ability to early detect the presence of active disease, hopefully before macroscopic evaluation, is particularly relevant for new drugs testing studies since ideally the effect of potentially therapeutic molecules is better assessed in small, well vascularized masses without necrosis. Therefore it is crucial to identify a suitable murine model of disease that can be accurately monitored by PET imaging.

Xenograft models present some limitations mainly related to the formation of a chimeric neoplastic tumour, to the need of an immunocompromised host and, in some cases, to the heterotopic site of tumour formation; nevertheless xenografts models have been widely employed, especially for drug testing studies, for their low cost and reproducibility. On the other hand, transgenic models are orthotopic but are characterized by an entirely murine tumour mass and are very expensive.

Karpas 299 xenograft murine model, expressing the NPM-ALK fusion gene, has been used in different studies investigating the role of novel molecules for lymphoma therapy [24-26]. To our knowledge there are no reports evaluating the imaging features of this lymphoma murine model and the metabolic changes of the tumour mass over time.

Aim of the present study was to assess if a xenograft model with a well established human ALCL cell line could be accurately monitored by small animal PET over time and if PET could be used to early assess the presence of the tumour and therefore proposed to select mice bearing tumours early in the course of the disease to promptly start the testing of a new drug.

MATERIALS AND METHODS

Cell culture

Human Anaplastic Large Cell Lymphoma Karpas 299 cell line (established from a 25 years old ALCL patient) was purchased from DSMZ (Germany) [1,27]. Cells were maintained in 90% RPMI medium 1640 supplemented with 10% FBS at $1.0-2.0 \times 10^6$ cells/ml (maximal density of about $2-3 \times 10^6$ cells/ml). Cells cultures were kept at 37 °C with 5% CO₂.

Karpas 299 immunological profile, as provided by DSMZ, includes: CD2 -, CD3 -, CD4 +, CD5 +, CD6 -, CD7 -, CD8 -, CD10 -, CD13 +, CD14 -, CD15 -, CD19 -, CD20 +, CD25 +, CD30 +, CD33 -, CD34 -, CD71 +, HLA-DR +, TCRalpha/beta -, TCRgamma/delta -. Cytogenetic analysis shows human hypodiploid karyotype with 14% polyploidy - 44(42-45)<2n>XY, -10, -22, t(1;17)(q22;p11), t(2;5)(p23;q35), del(6)(q23), der(13)t(13;?)(p12;?), der(14)t(14;22)(p12;q11), der(19)t(19;?)(q13;?), del(22)(q12) - expression of NPM-ALK fusion gene was detected by RT-PCR analysis.

Animal model

Eight six weeks-old severely immunocompromised NOD/SCID mice were used in the study. Animals were purchased from Charles Rivers Laboratories (Italy). Mice mean weight was 25.9gr (range 22-30gr). Animals were given food and drink ad libitum, manipulated under sterile conditions and closely monitored for their health at the Experimental Surgery Laboratory, Istituti Ortopedici Rizzoli. Karpas 299 cells growing exponentially were resuspended in PBS and inoculated into mice subcutaneously (1×10^7 cells/mouse in 150 uL FBS) at right flank level.

The whole experiment was approved by the Ethical Committee of the University of Bologna.

Tumour Imaging by FDG Small Animal PET

PET scans were carried out under sevoflurane (5%) anaesthesia (VetEquip Complete Anaesthesia System, Pleasanton, CA) and oxygen supplementation (1L/min). Each anaesthetised animal was injected with 20 MBq of ¹⁸F-FDG in the tail vein (injected volume <0.15ml) and subsequently allowed to wake up during the uptake time (60minutes). The

residual dose in the syringe was measured to verify the effective dose injected. At the end of the uptake time, PET image acquisition was performed with a Small Animal PET tomograph (GE eXplore Vista DR) in the anaesthetised mouse placed prone on the scanner bed. Total acquisition time was 15 minutes. Since the axial field of view was 4 cm, a single bed position was sufficient to cover the whole body. Once the scan was completed, the animal was allowed to wake up in a warmed recovery box.

Early PET imaging was obtained at 2 days from cells inoculation in 4/8 animals and at 4 days in the remaining 4/8 animals. Later scans were performed in all animals at 7, 14, 21, 28 days from cells injection.

FDG PET images were reconstructed iteratively (OSEM 2D) and read in three planes (axial, sagittal and coronal). The scan was considered positive if any area of increased non-physiologic FDG uptake was observed. Cold areas located at the centre of a tumour mass were interpreted as areas of necrosis. Semi-quantitative analysis was carried out in all cases using the tumour to background ratio (TBR), placing the target region of interest (ROI) in the most active tumour area and the background ROI in the contra-lateral subcutaneous tissue ($TBR = \text{Max Count in the target ROI} / \text{Mean count in the background ROI}$).

Histology evaluation

Pathological sections were obtained in all cases. Animals were sacrificed 30 days after tumour cells inoculation (6/8 cases). Autopsy was performed before the end of the study in the two animals that died during the experiment (one mouse died after the first PET and one animal died at 27 days from tumour cells injection). Pathology was used to confirm PET findings. In all cases the tumour was excised and samples from heart, lungs and peritoneum were obtained for histological evaluation. At macroscopic observation one mouse showed liver and kidney enlargement therefore liver and kidney samples were collected. In one case with all negative PET scans, samples were taken also from liver and intestine.

Formalin fixed tissue samples were embedded in paraffin and 5µm sections were cut and stained with hematoxylin and eosin.

RESULTS

Early PET evaluation after tumour cells injection (in 4/8 animals at 2 days and in the remaining 4/8 mice at 4 days) was negative in all cases. Subsequently small animal PET identified the presence of lymphoma in 6/8 (75%) mice. A pathologic FDG uptake at inoculation site was evident at 7 days after implantation in 4/8 (50%) mice and at 14 days in

2/8 (25%) animals. Of the remaining two animals, one died after the first PET scan and autopsy did not reveal the presence of the tumour; PET scans carried out in the other mouse were negative at all time-points.

In all cases PET detected the presence of viable tumour cells before macroscopic evaluation. Palpable tumours were observed at 14 days in 3/8 and at 21 days in 3/8 (overall mean 17.5days), therefore PET detected the tumour mass with an average of 8 days (range 7-14 days) in advance.

Serial PET documented a progressive increase in the metabolic activity of the tumour mass in all PET positive mice (Figure 1). In the latest scans, PET showed in 6/6 cases cold central lesion areas compatible with necrosis, secondary to tumour vascularisation incompetence.

The lesions mean TBR presented a greater increase in the first three weeks, especially between 7 and 14 days, while in the latest scans the trend tends to a plateau, reflecting the necrotic changes in the tumour mass (Figure 2).

Quite interestingly, in the two animals in which PET turned positive only at 14 days, the mean TBR at 14 days was higher (6.2) than the mean TBR observed in the animals that turned positive 7 days (4.4).

Pathology sections of the tumour samples (Figure 3) showed in all cases the presence of an aggressive tumour, with pleomorphic lymphoma cells presenting a high mitotic and apoptotic rate. In all animals the lesions presented a big central necrotic area. The tumour often infiltrated adjacent tissues (muscles, abdomen wall, fat, peritoneal vessels) and organs, including kidneys (in one case), liver (in two cases), intestine (one case) and lung (in five cases). The involved lungs presented diffuse lymphoma cells infiltration with sparse foamy macrophages that filled the alveolar spaces without evident fibrosis. The widespread lung involvement prevented any considerations regarding the pulmonary TBR changes over time.

Autopsy carried out in the single animal in which PET was negative at all time-points revealed the presence of a very small lymphoma infiltration embracing the trachea and esophagus with no macroscopically evident mass at neither tracheal nor at inoculation site.

DISCUSSION

Murine models of human cancer are valid tools to study tumour development over time and to test potentially curative new drugs. Xenograft models in particular are extensively used for new drugs testing for their low cost, reproducibility and similarities with human tumours.

In recent years different imaging modalities, traditionally used for humans, such as PET, CT, MRI, optical imaging and SPECT have been designed for animal research. For new drugs

testing small animal PET offers many advantages over anatomical imaging modalities that rely only on size criteria for the evaluation of therapy response. PET offers the advantage of non-invasively providing functional information of the tumour lesion and is therefore very accurate for the assessment of the metabolic changes consequent to drug administration. Moreover, PET can detect the presence of viable tumour cells at a very early stage and this feature can be particularly helpful for identifying animals with very small, well vascularized tumours, an ideal setting for testing new drugs. However, before testing a new molecule, it is crucial to assess the metabolic characteristics of the tumour over time and the earliest time-point when the lesion can be detected.

Much attention has been directed to therapeutic drugs aimed at down-regulating NPM-ALK fusion protein expression or inhibiting the NPM-ALK signalling cascade [28,29] and recently siRNA were used to specifically down-regulate NPM-ALK fusion protein expression in Karpas 299 cell line in vitro inducing decreased cell proliferation and increased apoptosis [30].

Therefore, we chose a murine xenograft model using a well established ALCL cell line, carrying the t(2;5) chromosome translocation, in order to evaluate tumour development over time by small animal PET.

In our sample, PET detected the presence of the tumour in almost all animals, identifying the earliest lesions at seven days after cells inoculation in the majority of cases; furthermore in all mice PET identified the tumour earlier than macroscopic evaluation (on average seven days in advance).

In fact PET was positive in 6/8 mice, while in the remaining two cases there was no lesion that PET could have detected (one mouse died very early, the other did not develop a mass at inoculation site).

These data are particularly promising underlying the possibility to detect the presence of a very small tumour at an early stage, an ideal setting for new drugs setting. Our results are quite interesting when compared with the ones obtained by Jundt et al, studying the same model macroscopically [26]. The authors obtained palpable lesions between one and two weeks, reaching an average tumour volume of 32.7mm^3 at 16 days, while in our series a palpable mass was evident between two and three weeks. Differences in tumour cells phase of growth at the time of inoculation may have accounted for differences in time of formation of a palpable mass. Moreover, patterns of differential tumour growth may exist among different animals as reported by Sato et al in five SCID mice injected with Karpas 299 intraperitoneally [31].

Tumour lesions presented a progressive increased metabolic activity, as expressed by mean TBR variations, especially in the first three weeks. Afterwards, the TBR reaches a plateau which reflects the necrotic changes evident on the latest PET scans in the central areas of the tumour mass. The higher mean TBR value of the animals with first positive PET at 14 days compared with those with first positive PET at seven days, suggested the need to further assess one week PET-negative animals between 7 and 14 days, since it is likely that the tumour lesion may have been detected earlier.

Pathologic examination showed a widespread tissue distribution including lungs, liver, kidneys, intestine, as well as adjacent fat and muscles. The widespread distribution of lymphoma cells in the alveolar spaces was the major reason why we chose the background ROI in the contra-lateral subcutaneous tissue instead of the lungs.

In one case PET was negative at all time-points while autopsy revealed the presence of tumour cells at tracheal level without a macroscopically evident tumour mass. Although a localization of lymphoma cells at head and neck level has been reported after intravenous Karpas 299 cells administration [32], it seems unlikely this is the case, since autopsy did not reveal any other site of tumour involvement that could be expected after cells intravenous injection. One possible explanation for this unusual localization could be advocated to a mistaken cells injection directly at mediastine level.

CONCLUSIONS

In this ALCL xenograft murine model small animal PET allowed the detection of tumour lesions before macroscopic evaluation at a very early stage. The selection of tumour bearing animals early in the course of the disease can be useful for new drugs testing studies and for monitoring tumour response to therapy.

FUTURE DIRECTIONS..

Since small animal PET provided a good characterization of this tumour model, in the next future small animal PET will be used to assess tumour response to experimental anti-proliferative drugs.

REFERENCES SECTION 3

1. Falini B. Anaplastic large cell lymphoma: pathological, molecular and clinical features. Br J Haematol. 2001 Sep;114(4):741-60.

2. Stein H, Foss HD, Durkop H, Marafioti T, Delsol G, Pulford K, et al. CD30(+) anaplastic large cell lymphoma: a review of its histopathologic, genetic, and clinical features. *Blood*. 2000 Dec 1;96(12):3681-95.
3. O'Doherty MJ, Hoskin PJ. Positron emission tomography in the management of lymphomas: a summary. *Eur J Nucl Med Mol Imaging* 2003; 30 (s1): s128-s130.
4. Hoskin PJ. PET in lymphoma: what are the oncologist's need. *Eur J Nucl Med Mol Imaging* 2003; 30 (s1): s37-s41.
5. Delbeke D, Martin WH, Morgan DS, Kinney MC, Feurer I, Kovalsky E, et al. 2-deoxy-2-[F-18]fluoro-D-glucose imaging with positron emission tomography for initial staging of Hodgkin's disease and lymphoma. *Mol Imaging Biol* 2002; 4(1): 104-114.
6. Kostakoglu L, Coleman M, Leonard JP, Kuji I, Zoe H, Goldsmith SJ. PET predicts prognosis after 1 cycle of chemotherapy in aggressive lymphoma and Hodgkin's disease. *J Nucl Med*. 2002; 43(8): 1018-27.
7. Spaepen K, Stroobants S, Dupont P, Vandenberghe P, Thomas J, de Groot T, et al. Early restaging positron emission tomography with (18)F-fluorodeoxyglucose predicts outcome in patients with aggressive non-Hodgkin's lymphoma. *Ann Oncol*. 2002; 13(9): 1356-63.
8. Guay C, Lepine M, Verrault J, Bernard F. Prognostic value of PET using 18F-FDG in Hodgkin's disease for posttreatment evaluation. *J Nucl Med* 2003; 44: 1225-1231.
9. Weihrauch MR, Re D, Scheidhauer K, Ansen S, Dietlein M, Bischoff S et al. Thoracic positron emission tomography using 18F-fluorodeoxyglucose for the evaluation of residual mediastinal Hodgkin disease. *Blood* 2001; 98 (10): 2930-2934.
10. Lavelly WC, Delbeke D, Greer JP, Morgan DS, Byrne DW, Price RR, et al. FDG PET in the follow-up management of patients with newly diagnosed Hodgkin and non-Hodgkin lymphoma after first-line chemotherapy. *Int J Radiat Oncol Biol Phys*. 2003; 57(2): 307-15.
11. Romer W, Schwaiger M. Positron Emission Tomography in Diagnosis and Therapy Monitoring of Patients with Lymphoma. *Clin Positron Imaging*. 1998; 1(2): 101-110.
12. Massoud TF, Gambhir SS. Molecular imaging in living subjects: seeing fundamental biological processes in a new light. *Genes Dev*. 2003 Mar 1;17(5):545-80.
13. Blasberg RG. In vivo molecular-genetic imaging: multi-modality nuclear and optical combinations. *Nucl Med Biol*. 2003 Nov;30(8):879-88.
14. Deroose CM, De A, Loening AM, Chow PL, Ray P, Chatziioannou AF, et al. Multimodality imaging of tumor xenografts and metastases in mice with combined small-animal PET, small-animal CT, and bioluminescence imaging. *J Nucl Med*. 2007 Feb;48(2):295-303.

15. Blasberg RG, Tjuvajev JG. Molecular-genetic imaging: current and future perspectives. *J Clin Invest.* 2003 Jun;111(11):1620-9.
16. Blasberg RG. Molecular imaging and cancer. *Mol Cancer Ther.* 2003 Mar;2(3):335-43.
17. Herschman HR. Micro-PET imaging and small animal models of disease. *Curr Opin Immunol.* 2003 Aug;15(4):378-84.
18. Phelps ME. PET: the merging of biology and imaging into molecular imaging. *J Nucl Med.* 2000 Apr;41(4):661-81.11.
19. Ritman EL. Micro-computed tomography-current status and developments. *Annu Rev Biomed Eng.* 2004;6:185-208.
20. Gouvain KM, Garbow JR, Song SK, Hirbe AC, Weilbaecher K. MRI detection of early bone metastases in b16 mouse melanoma models. *Clin Exp Metastasis.* 2005;22(5):403-11.
21. Kulbersh BD, Duncan RD, Magnuson JS, Skipper JB, Zinn K, Rosenthal EL. Sensitivity and specificity of fluorescent immunoguided neoplasm detection in head and neck cancer xenografts. *Arch Otolaryngol Head Neck Surg.* 2007 May;133(5):511-5.
22. Tai YC, Ruangma A, Rowland D, Siegel S, Newport DF, Chow PL, et al. Performance evaluation of the microPET focus: a third-generation microPET scanner dedicated to animal imaging. *J Nucl Med.* 2005 Mar;46(3):455-63.
23. Aliaga A, Rousseau JA, Cadorette J, Croteau E, van Lier JE, Lecomte R, et al. A small animal positron emission tomography study of the effect of chemotherapy and hormonal therapy on the uptake of 2-deoxy-2-[F-18]fluoro-D-glucose in murine models of breast cancer. *Mol Imaging Biol.* 2007 May-Jun;9(3):144-50.
24. Tian ZG, Longo DL, Funakoshi S, Asai O, Ferris DK, Widmer M, et al. In vivo antitumor effects of unconjugated CD30 monoclonal antibodies on human anaplastic large-cell lymphoma xenografts. *Cancer Res.* 1995 Nov 15;55(22):5335-41.
25. Ho L, Aytac U, Stephens LC, Ohnuma K, Mills GB, McKee KS, et al. In vitro and in vivo antitumor effect of the anti-CD26 monoclonal antibody 1F7 on human CD30+ anaplastic large cell T-cell lymphoma Karpas 299. *Clin Cancer Res.* 2001 Jul;7(7):2031-40.
26. Jundt F, Raetzl N, Muller C, Calkhoven CF, Kley K, Mathas S, et al. A rapamycin derivative (everolimus) controls proliferation through down-regulation of truncated CCAAT enhancer binding protein {beta} and NF- κ B activity in Hodgkin and anaplastic large cell lymphomas. *Blood.* 2005 Sep 1;106(5):1801-7.
27. Fischer P, Nacheva E, Mason DY, Sherrington PD, Hoyle C, Hayhoe FG, et al. A Ki-1 (CD30)-positive human cell line (Karpas 299) established from a high-grade non-Hodgkin's

lymphoma, showing a 2;5 translocation and rearrangement of the T-cell receptor beta-chain gene. *Blood*. 1988 Jul;72(1):234-40.

28. Piva R, Chiarle R, Manazza AD, Taulli R, Simmons W, Ambrogio C, et al. Ablation of oncogenic ALK is a viable therapeutic approach for anaplastic large-cell lymphomas. *Blood*. 2006 Jan 15;107(2):689-97.

29. Voena C, Conte C, Ambrogio C, Boeri Erba E, Boccalatte F, Mohammed S, et al. The tyrosine phosphatase Shp2 interacts with NPM-ALK and regulates anaplastic lymphoma cell growth and migration. *Cancer Res*. 2007 May 1;67(9):4278-86.

30. Hsu FY, Zhao Y, Anderson WF, Johnston PB. Downregulation of NPM-ALK by siRNA Causes Anaplastic Large Cell Lymphoma Cell Growth Inhibition and Augments the Anti Cancer Effects of Chemotherapy In Vitro. *Cancer Invest*. 2007 Jun;25(4):240-8.

31. Sato T, Yamochi T, Yamochi T, Aytac U, Ohnuma K, McKee KS, et al. CD26 regulates p38 mitogen-activated protein kinase-dependent phosphorylation of integrin beta1, adhesion to extracellular matrix, and tumorigenicity of T-anaplastic large cell lymphoma Karpas 299. *Cancer Res*. 2005 Aug 1;65(15):6950-6.

32. Zhang M, Yao Z, Patel H, Garmestani K, Zhang Z, Talanov VS, et al. Effective therapy of murine models of human leukemia and lymphoma with radiolabeled anti-CD30 antibody, HeFi-1. *Proc Natl Acad Sci U S A*. 2007 May 15;104(20):8444-8.

FIGURES SECTION 3

Figure 3.1. Serial 18F-FDG small animal PET images of ALCL development after implantation of human Karpas 299 cells. Early PET scan was negative (2days) while PET performed at 7 days from tumour cells implantation showed the presence of a pathologic FDG uptake area at inoculation site. The metabolic activity of the mass progressively increased over time (14,21 days) while later scans showed cold areas in the context of the lesion reflecting the presence of necrotic areas (21,28 days).

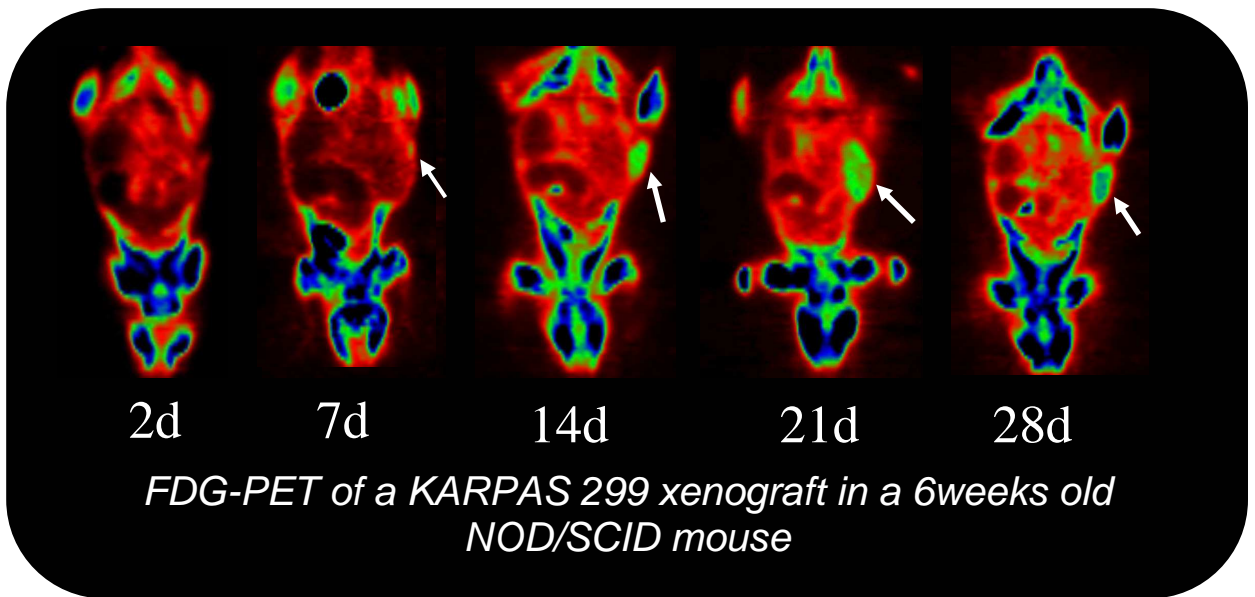


Figure 3.2. Tumour to background (TBR) variations over time in PET-positive tumour bearing animals showed a greater increase in the first three weeks. The TBR trend tended to a plateau at later time-points reflecting the presence of central necrotic areas.

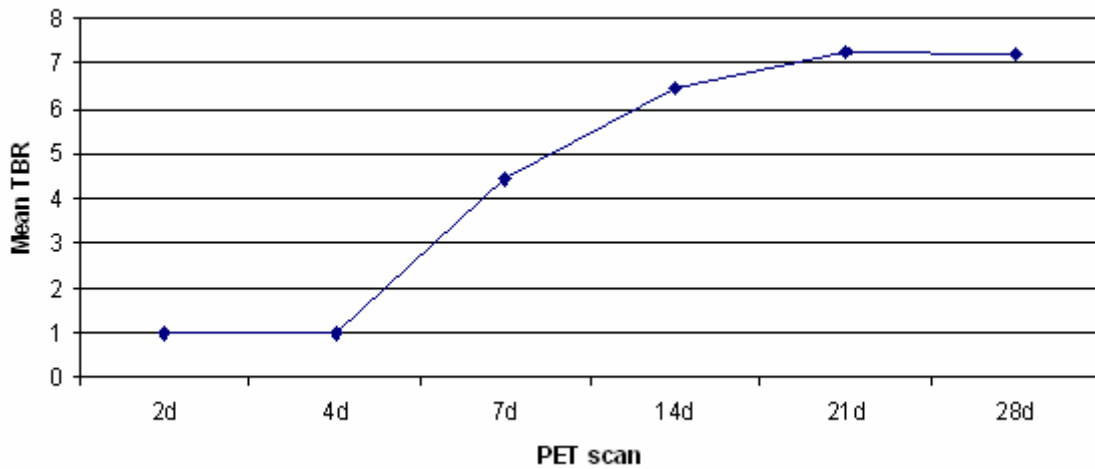
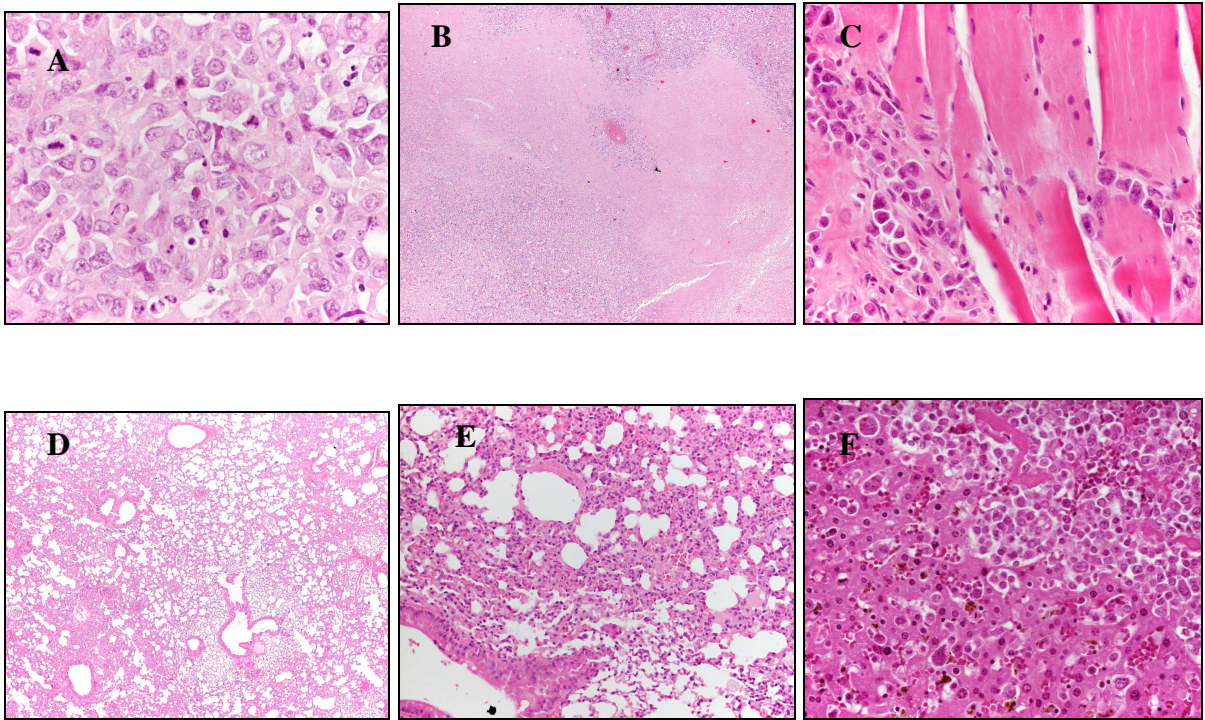


Figure 3.3. Pathologic sections of a NOD/SCID mouse inoculated with the human ALCL Karpas 299 cell line. The tumour mass showed highly pleomorphic lymphoma cells with a high mitotic and apoptotic rate (A, 60x) and a big central necrotic area (B, 4x). The tumour was very aggressive, infiltrating adjacent muscles (C, 40x), the lungs (D, 4x; E, 20x) and the liver (F, 40x).



SECTION 4

SMALL ANIMAL PET APPLICATIONS IN CARDIOLOGY (rat model of heart infarction)

INTRODUCTION

Heart disease is the most frequent cause of morbidity and mortality in the US and most western countries. Until recently, treatment of heart disease has been targeted on the anatomic and physiologic effects (coronary artery bypass surgery, percutaneous transluminal coronary angioplasty) for relieving obstructive coronary atherosclerosis. The recent advances in imaging technology enable innovative research and significant improvements in cardiovascular therapy. Non-invasive imaging of the integrative functions of molecules, genes, and cells in intact living subjects is now possible and provides a sophisticated evaluation of the disease process [1]. Multiple imaging technologies have been developed or adapted from human use for this purpose, including positron emission tomography (PET), single-photon emission computed tomography (SPECT), magnetic resonance imaging (MRI), computed tomography (CT) targeted contrast ultrasound, bioluminescence, fluorescence, and near-infrared fluorescence (NIRF).

Potential applications of molecular imaging in cardiovascular medicine include the analysis of vulnerable plaques, heart failure, neuro-hormonal dysfunction, myocardial metabolism, stem cell engraftment, protein-protein interactions, and angiogenesis.

One of the main goals of research in cardiology is to identify an effective treatment strategy that could induce infarcted myocardial regeneration: cell transplantation to repair or regenerate injured myocardium (cellular cardiomyoplasty) has been proposed as a new approach for treatment [2,3]. Many pre-clinical studies tried to address this issue, much remains to be understood about this methodology, as well as its possible applications in the clinic. For example, controversies exist over the specific cells to be used, the dosages needed for tissue repair, how cells will affect the electrical activity of the myocardium, and even whether the cells can improve myocardial function after transplantation [4].

Among all cell types used in the pre-clinical setting, only stem cells derived from the bone marrow, endothelial cells precursors and skeletal myoblasts have been used in clinical trials, mainly as a consequence of their availability, resistance to ischemia and ethical issues (compared to the use of human embryonic or fetal cells) [5,6,7].

Despite the initial enthusiasm of in-vitro and pre-clinical in-vivo studies, doubts have been raised about the potential of bone marrow stem cells to integrate into the myocardium and

differentiate into cardiac-like cells [8,9,10]. Autologous skeletal muscle precursors cells have been proposed as cell sources but there is no direct evidence of their ability to integrate in the myocardium from a morphological and functional point of view [8,11,12].

Factors that are indirectly correlated with cells engraftment include the cells paracrine activity with effects on the surrounding necrotic tissue and the cells ability to promote the release of angiogenic factors that can induce extra-cellular matrix remodelling (lower collagen deposition with subsequent increase in myocardial compliance) [13,14].

Another crucial issue is the route of cells administration. Traditionally, the most popular method for cell transplantation into the heart is direct intramuscular injection, which allows the selective cell delivery into either normal or infarcted myocardium [15,16]. The main limitation of this is the mechanical injury and subsequent acute inflammation that results in poor survival of grafted cells and myocardial damage [11,12,17]. Furthermore, myocardial precursors cells infused by this method usually produce localized islet-like formations, isolated from the native myocardium [11]. Cells delivery via the intra-coronary route presents theoretical advantages over direct intramuscular injection allowing global cell dissemination within the myocardium [17,18]. This method is also likely to result in less myocardial and graft injury. Recent evidence demonstrated that myocardial precursors cells grafted by antegrade intra-coronary infusion successfully disseminated throughout cardiac layers, proliferated, differentiated, and integrated into host myocardium in rat [17,18]. Moreover, antegrade intra-coronary myocardial precursors cells transplantation resulted in cardiac function improvement in rats with doxorubicin-induced heart failure [19]. This route has recently been applied for infusion of bone marrow stem cells into infarcted human hearts [2]. However, some authors reported that antegrade intra-coronary infusion is not the best administration route to deliver cells to ischemic or infarcted areas and is associated with a risk of coronary embolism [17,18,19]. A novel approach consists in the retrograde intra-coronary delivery, that is an efficient way to administer cardioplegic solutions, peptides, and vectors for gene therapy into the myocardium of laboratory animal [20-23]. Emigration of inflammatory cells into the myocardial interstitium is known to take place at post-capillary venules rather than at arterioles or capillaries [24]. Retrograde intra-coronary infusion might offer a safer and more efficient cell dissemination within the myocardium even in ischemic or infarcted areas where antegrade arterial delivery has been reported to have limited efficacy.

Over the past decades, nuclear medicine has gained a relevant role for the assessment of cardiologic disorders in humans. In particular, PET has contributed significantly to advances in understanding heart physiology and pathophysiology (in-vivo quantitation of heart

perfusion, heart viability) and pre-clinical PET is nowadays an accurate tool for the assessment of heart function.

Direct molecular imaging allows the evaluation of myocardial viability and heart perfusion using tracers such as ^{18}F -FDG, ^{82}Rb , ^{13}N -ammonia, ^{15}O -water. Although these techniques found several applications in pre-clinical imaging, they are all widely used in the human patient. A different approach is reporter imaging that consists of in-vitro genetic labelling of target cells that are subsequently injected in the animal and detected by small animal PET (e.g. HSV1-FHBG). Reporter imaging finds application for the in-vivo study of stem cells, a potential therapeutic strategy for the regeneration of infarcted heart.

Imaging of molecular markers (such as VEGF, integrins, annexins) that are over-expressed only in specific pathologic conditions.

From a clinical point of view, the assessment of myocardial viability in patients with decreased left ventricular function is a very important issue since patients with evidence of viability that undergo revascularization have better survival compared to those who receive medical management [25-28] and a significant proportion of patients with depressed left ventricular function have evidence of viability and can have improvement in left ventricular function following revascularization [29,30].

To assess myocardial availability, the most commonly used tracer is ^{18}F -FDG in both clinical and pre-clinical setting [31]. Viable myocardial cells (although stunned or ibernated) present an increased ^{18}F -FDG uptake, depending on glucose and insulin serum levels [32-34]. Therefore ^{18}F -FDG is the tracer of choice for the assessment of viable myocardium.

However, a fundamental question is how to measure the infarcted area in the laboratory animal, in order to perform comparative measures over time. It is important to note that the aim of performing ^{18}F -FDG PET is different in the human patient and in the laboratory animal. In the clinical setting, it is crucial to identify those patients who would benefit more from a re-vascularization: especially when associated to a perfusion study, ^{18}F -FDG PET allows to predict post-revascularization improvement in left ventricular function in case of mismatch between blood flow (^{82}Rb ; ^{15}O water; ^{13}N ammonia) and FDG metabolism. In the pre-clinical setting it is fundamental to measure the volume of viable myocardium in order to assess the effect of experimental therapies (such as regenerative therapies using stem cells).

In the present study, the preliminary data of an on-going study to evaluate the volume of viable myocardium in infarcted rats are described in detail. The role of small animal PET to assess the effects of an experimental regenerative treatment (cellular cardiomyoplasty+infusion of relaxin) to induce myocardial regeneration is also described.

METHODS

Animal model

We surgically induced a left ventricular anterior infarction through occlusion of the LAD (left anterior descendent) coronary artery (general anaesthesia: 50mg/kg i.p. pentobarbital; tracheal cannula: 14 Gauge; volume controlled mechanical ventilation: FiO₂ 80-100%, FR 45/min, I:E=0.7, PEEP 0,5cmH₂O; descendant anterior coronary artery ligation after the first diagonal branch in order to minimize the extension of the induced infarct and to obtain a chronic cardiac insufficiency with a cardiac output of 30-35%) in 16 non-diabetic Wistar rats (200-300gr). All surgical procedures were performed at the Experimental Surgery Laboratory, University of Florence. During the surgical procedure, blood pressure was invasively monitored at femoral artery level. Immediately after surgery, animals were allowed to recover in a warm box with increased oxygen flow.

Infarcted animals were then divided into 2 groups: Cases (8 animals) and Controls (8 animals).

Control animals were studied by 18F-FDG PET at 4 wks, 5 wks and 7 wks after surgery.

Case rats were studied 4 wks after surgery and then treated by i.v. infusion of mouse myoblasts (C2C12 cell line) genetically engineered to produce relaxin (2×10^6 cells/100gr of body weight, suspended in 1ml of saline, were infused in 1 minute at coronary vein level), associated with i.p. implantation of a osmotic micro pumping device constantly releasing relaxin (5 mg/kg b.wt./day). This group was studied by small animal PET 1 wk, 2 wks and 5 wks after cell grafting.

Oral ciclosporin (15mg/kg) was administered in all animals to obtain immunosuppression after myoblasts/placebo infusion.

Cells cultures

Cells were cultured and engineered at the Unit of Cardiac Surgery, University of Florence. Mouse myoblasts (C2C12 cell line) were cultured in DMEM with 10% fetal calf serum, gentamicin-streptomycin (100U/ml) and maintained at 37°C and 5% CO₂. Cells were genetically engineered to produce relaxin using a lenti-viral vector (containing the human gene RLN2, encoding for relaxin, and a reporter gene called eGFP, encoding for a fluorescent protein) [35]. These cells, called C212/RLX, were administered by retrograde intra-coronary infusion in Group 2 rats and were able to produce relaxin at a concentration of 1.8ng/ml,

pharmacologically active and measurable by ELISA. Cells clones were analyzed by fluorescence microscopy and flow cytometry to assess the expression of eGFP.

Imaging by 18F-FDG PET

All animals were i.p. administered a 5% glucose solution before the PET scan in order to increase insulin blood levels. PET scans were carried out under sevoflurane (5%) anaesthesia (VetEquip Complete Anaesthesia System, Pleasanton, CA) and oxygen supplementation (1L/min).

Small animal 18F-FDG PET (GE eXplore Vista DR) was performed after 1 month, 2 months and 3 months from myocardial infarction under standard procedures (18F-FDG tail vein injected dose 45MBq, uptake time 30min, acquisition time 20min, reconstruction OSEM2D). Animals were allowed to wake up during uptake time in a warm recovery box.

In order to evaluate the volume of viable myocardium, we semi-automatically draw a volume of interest (VOI) over the left viable ventricle and used the small animal PET workstation software to calculate a volume including all surrounding areas presenting the same metabolic activity. In this way we obtained a measure of the viable myocardium that is complimentary to the infarcted area. We used this method to calculate the volume of viable myocardium scan by scan. Statistical significance between experimental values was determined by t testing, and differences were considered significant at $p < 0,005$.

PRELIMINARY RESULTS

The mean volume measured in cases and controls is shown in Figure 4.1. Treated animals had a mean increase of viable myocardium of 7%, 35% and 26% at 1, 2 and 5 wks after cell infusion, respectively (Figure 4.2). The control group showed a mean increase of 14% and 10% at 5 and 7 wks after surgery, respectively. The difference in the mean viable myocardium between cases and controls was statistically significant at the third scan ($p=0,003$). Comparing the volume of viable myocardium rat by rat, case rats presented a significant increase in viable myocardium between the second and first scan ($p=0,04$) and between the third and first scan ($p=0,03$) while controls presented a significant difference only between the second and first scan ($p=0,02$).

Pathological examination of the myocardium is on-going to investigate the effects of myoblasts cell therapy.

DISCUSSION OF PRELIMINARY RESULTS

Nuclear medicine has a relevant role in the assessment of heart pathophysiology in humans. With the advent of small animal PET tomographs, it is now possible to perform PET in rodents with heart disease.

In our preliminary experience we developed a protocol in order to standardize the measure of viable myocardium assessed by small animal PET. A rat model of surgically induced heart infarction was serially studied by small animal PET with FDG at baseline (after ligation of the LAD) and at serial time-points in both controls (placebo) and rats treated with infusion of myoblasts engineered to produce relaxin associated with the implantation of a micro-pumping device releasing relaxin.

Our preliminary data showed that small animal PET with ¹⁸F-FDG is an accurate tool to study the volume of viable myocardium after infarction in laboratory animals and to assess the response to regenerative treatment.

The mean volume of viable myocardium was significantly higher in animals treated with myoblasts infusion associated with relaxin administration compared with control animals treated with placebo. The slight increase in the control at the second PET scan can be explained with the physiologic animal increase in body weight. In fact a major limit in this protocol is that performing serial PET scans over time the physiologic increase of the heart (in both cases and controls) has to be taken into account (especially since the heart does not increase proportionally to body weight). Pathological examination of the myocardium will be carried out to investigate the effects of myoblasts cell therapy and observe if there are any correlation with the total weight of the heart at the time of PET scan.

At present, it is quite easy to measure the infarcted area in the human patient, since appropriate software are already available. In the pre-clinical setting, the issue is still debated although some authors reported that the extent of the infarcted area induced in the mouse or in the rat measured with manual or semi-automated tools on PET images is strictly correlated with the pathological data [36]. In our protocol we measured the viable myocardium drawing a small volume of interest in the viable myocardium and used the PET workstation software to include the surrounding areas with the same metabolic activity in the volume of interest. In this way we obtained a parameter that could be used in longitudinal studies with the aim to assess the response to treatment.

Another issue is to standardize myocardial glucose uptake in the animals. To overcome this problem, we administered each animal an i.p. glucose load 30 minutes before the PET scan in order to induce a shift of myocardial metabolism towards glucose consumption (in response

to the increased insulin serum levels). In this way we obtained a high uptake in the heart that allowed an accurate and standardized measure of the viable myocardium.

FUTURE DIRECTIONS..

As already said these are just preliminary results of a protocol that also includes in the next future the assessment of the effects of relaxin and cardiomyoplasty alone in two additional groups of animals that will be studied by small animal PET following the same procedure described above. In this way we will be able to derive conclusions on the role of relaxin and cardiomyoplasty, associated or alone, in the increase of viable myocardium. In fact, some authors have suggested that relaxin may have a role in promoting the regeneration of ischemic heart by inducing modifications in the extra-cellular matrix that would favour the homing and local proliferation of administered stem cells [37-39]. Moreover, relaxin could influence blood local flow promoting myoblasts survival and supporting their growth [3,40,41].

REFERENCES SECTION 4

1. Wu JC, Narula J. Molecular imaging in cardiology. *Current Opinion in Biotechnology* 2007, 18:1-3.
 2. Strauer BE, Kornowski R. Stem cell therapy in perspective. *Circulation*. 2003;107:929–934.
 3. Taylor DA, Atkins BZ, Hungspreugs P, et al. Regenerating functional myocardium: improved performance after skeletal myoblast transplantation. *Nature Med*. 1998;4:929–933.
 4. Taylor DA. Cellular cardiomyoplasty with autologous skeletal myoblasts for ischemic heart disease and heart failure. *Curr Control Trials Cardiovasc Med*. 2001; 2(5): 208–210
- Aggiungi ref in viola
5. Pagani FD, Dersimonian H, Zawadzka A, Wetzel K, Edge ASB, Jacoby DB, Dinsmore JH, Wright S, Arets TH, Eisen HJ, Aaronson KD. Autologous skeletal myoblast transplanted to ischemia damaged myocardium in human. *J Am Coll Cardiol*. 2003; 41:879-888.
 6. Kim BK, Tian H, Prasonsukarm K, Wu J, Angoulvant D, Wnendt S, Muhs A, Spitkovsky D, Li RK. Cell transplantation improves ventricular function after a myocardial infarction: a preclinical study of human unrestricted somatic stem cells in a porcine model. *Circulation*. 2005; 112:I-96-I-104.
 7. Ye L, Haider HK, Sim EK. Adult stem cells for cardiac repair: choice between skeletal myoblasts and bone marrow stem cells. *Exp Biol Med*. 2006; 231:8-19.

8. C.E. Murry, L.J. Field, P. Menaschè. Cell based cardiac repair. Reflections at the 10-year point. *Circulation* 2005; 112: 3174-3183.
9. Murry CE, Soompa MH, Reinecke H, Nakajima H, Nakajima HO, Rubart M, Pasumarthi KB, Virag JJ, et al. Haematopoietic stem cells do not transdifferentiate into cardiac myocytes in myocardial infarcts. *Nature* 2004; 428: 664-668.
10. Sanchez PL, San Roman JA, Villa A, Fernandez E, Fernandez Aviles F. Contemplating the bright future of stem cell therapy for cardiovascular disease. *Nature Clinical Practice*. 2006; 3:S138-S151.
11. Reinecke H, Murry CE. Transmural replacement of myocardium after skeletal myoblast grafting into the heart: too much of a good thing? *Cardiovas pathol*. 2000; 9: 337-344.
12. Leobon B, Garcin I, Menaschè P, Vilquin J-T, Audinat E, Charpak S. Myoblast transplanted into rat infarcted myocardium are functionally isolated their host. *PNAS*. 2003; 100: 7808-7811.
13. Matsumoto R, Omura T, Yoshiyama M, Hayashi T, Inamoto S, Koh KR, Ohta K, Izumi Y...et al. Vascular endothelial growth factor expressed in mesenchymal stem cell transplantation for the treatment of acute myocardial infarction. *Atheroscler Thromb Vasc Biol*. 2005; 25: 1168-1173.
14. Berry MF, Engler AJ, Woo YP, Pirolli TJ, Bish LT, Jayasankar V, Morine KJ, Gardner TJ, Disher DE, Sweeney HL. Mesenchymal stem cell injection after myocardial infarction improves myocardial compliance. *Am J Physiol heart Circ Physiol*. 2006; H2196-H2203.
15. Menasche P, Hagege AA, Scorsin M, et al. Myoblasts transplantation for heart failure. *Lancet*. 2001;357:279-280.
16. Muller-Ehmsen J, Whittaker P, Kloner RA, et al. Survival and development of neonatal rat cardiomyocytes transplanted into adult myocardium. *J Mol Cell Cardiol*. 2002;34:107-116.
17. Robinson SW, Cho PW, Levitsky HI, et al. Arterial delivery of genetically labelled skeletal myoblasts to the murine heart: long-term survival and phenotypic modification of implanted myoblasts. *Cell Transplantation*. 1996;5:77-91.
18. Suzuki K, Brand NJ, Smolenski RT, et al. Development of a novel method for cell transplantation through the coronary artery. *Circulation*. 2000;102:III359-III364.
19. Suzuki K, Murtuza B, Suzuki N, et al. Intra-coronary infusion of skeletal myoblasts improves cardiac function in doxorubicin-induced heart failure. *Circulation*. 2001;104:I213-I217.

20. Ruengsakulrach P, Buxton BF. Anatomic and hemodynamic considerations influencing the efficiency of retrograde cardioplegia. *Ann Thorac Surg*. 2001;71:1389–1395.
21. von Degenfeld G, Raake P, Kupatt C, et al. Selective pressure-regulated retroinfusion of fibroblast growth factor-2 into the coronary vein enhances regional myocardial blood flow and function in pigs with chronic myocardial ischemia. *J Am Coll Cardiol*. 2003;42:1120–1128.
22. Boekstegers P, von Degenfeld G, Giehl W, et al. Myocardial gene transfer by selective pressure-regulated retroinfusion of coronary veins. *Gene Ther*. 2000;7:232–240.
23. Kupatt C, Wichels R, Deiss M, et al. Retroinfusion of NFkappaB decoy oligonucleotide extends cardioprotection achieved by CD18 inhibition in a preclinical study of myocardial ischemia and retroinfusion in pigs. *Gene Ther*. 2002;9:518–526.
24. MacSween RNM, Whaley K. Inflammation, healing and repair. *Muir's textbook of pathology*, 13th ed. London: Edward Arnold; 1992:112–165.
25. Pigott JD, Kouchoukos NT, Oberman A, et al. Late results of surgical and medical therapy for patients with coronary artery disease and depressed left ventricular function. *J Am Coll Cardiol* 1985;5:1036-45.
26. Marwick TH. The viable myocardium: epidemiology, detection, and clinical implications. *Lancet* 1998;351:815-9.
27. Acampa W, Petretta M, Spinelli L, et al. Survival benefit after revascularization is independent of left ventricular ejection fraction improvement in patients with previous myocardial infarction and viable myocardium. *Eur J Nucl Med Mol Imaging* 2005;32:430-7.
28. Meluzin J, Cerny J, Spinarova L, et al. Prognosis of patients with chronic coronary artery disease and severe left ventricular dysfunction. The importance of myocardial viability. *Eur J Heart Fail* 2003;5:85-93.
29. Bonow RO, Dilsizian V. Thallium 201 for assessment of myocardial viability. *Semin Nucl Med* 1991;21:230-41.
30. Schinkel AF, Bax JJ, Sozzi FB, et al. Prevalence of myocardial viability assessed by single photon emission computed tomography in patients with chronic ischaemic left ventricular dysfunction. *Heart* 2002;88:125-30.
31. Tillisch J, Brunken R, Marshall R, et al. Reversibility of cardiac wall-motion abnormalities predicted by positron tomography. *N Engl J Med* 1986;314:884-8.
32. Marwick TH, MacIntyre WJ, Lafont A, et al. Metabolic responses of hibernating and infarcted myocardium to revascularization. A follow-up study of regional perfusion, function, and metabolism. *Circulation* 1992;85:1347-53.

33. Gerber BL, Vanoverschelde JL, Bol A, et al. Myocardial blood flow, glucose uptake, and recruitment of inotropic reserve in chronic left ventricular ischemic dysfunction. Implications for the pathophysiology of chronic myocardial hibernation. *Circulation* 1996;94:651-9.
34. Tamaki N, Yonekura Y, Yamashita K, et al. Positron emission tomography using fluorine-18 deoxyglucose in evaluation of coronary artery bypass grafting. *Am J Cardiol* 1989;64:860-5.
35. Hudson P, Haley J, John M, Cronk M, et al. Structure of a genomic clone encoding biologically active human relaxin. *Nature* 1983; 301: 628-631.
36. Stegger L, Hoffmeier AN, Schäfers KP, Hermann S, Schober O, Schäfers MA, Theilmeier G. Accurate noninvasive measurement of infarct size in mice with high-resolution PET. *J Nucl Med.* 2006 Nov;47(11):1837-44.
37. Osheroff P. L, Cronin M.J and Lofgren J.A. Relaxin binding in the rat heart atrium. *Proc. Natl. Acad. Sci.* 1992 USA 89:2384-2388.
38. Dschietzig T, Richter C, Bartsch C, Laule M, Ambruster F, Baumann G, Stangl K. The pregnancy hormone relaxin is a player in human heart failure. *2001 FASEB J.*15:2187-2195.
39. Bani-Sacchi T, Bigazzi M, Bani D, Mannaioni PF, Masini E. Relaxin-induced increased coronary flow through stimulation of nitric oxide production. *Br J Pharmacol.* 1995 Sep;116(1):1589-94.
40. Bani-Sacchi T, Bigazzi M, Bani D, Mannaioni PF, Masini E. Relaxin-induced increased coronary flow through stimulation of nitric oxide production. *Br J Pharmacol.* 1995 Sep;116(1):1589-94.
41. Formigli L, Francini F, Tani A, Squecco R, Nosi D, Polidori L, Nistri S, Chiappini L, Cesati V, Pacini A, Perna AM, Orlandini GE, Zecchi Orlandini S, Bani D. Morphofunctional integration between skeletal myoblasts and adult cardiomyocytes in coculture is favored by direct cell-cell contacts and relaxin treatment. *Am J Physiol Cell Physiol.* 2005 Apr;288(4):C795-804.

FIGURES SECTION 4

Figure 4.1

Mean volume of viable myocardium in infarcted rats: cases (treated with myoblasts engineered to produce relaxin and relaxin administration by an osmotic micro-pumping) vs control animals (placebo). Treated animals had a mean increase of viable myocardium of 7%, 35% and 26% at 1, 2 and 5 wks after cell infusion, respectively. The control group showed a mean increase of 14% and 10% at 5 and 7 wks after surgery, respectively.

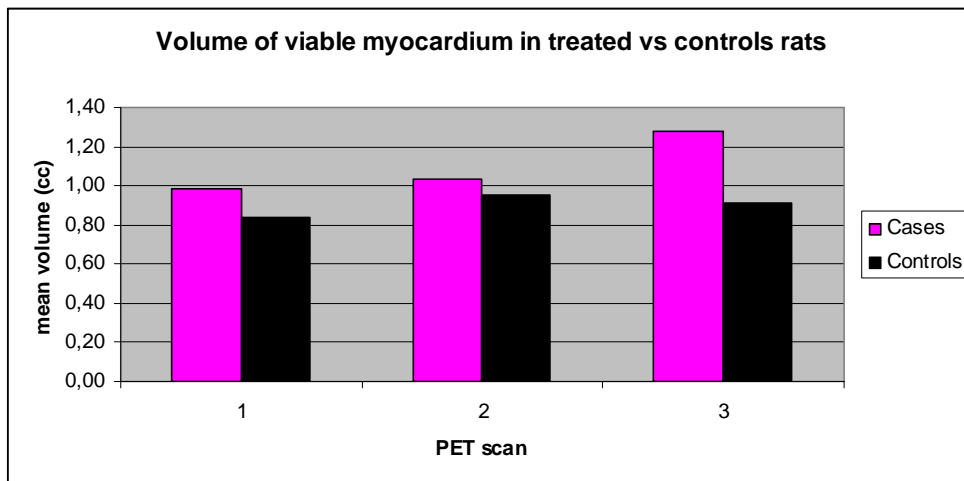
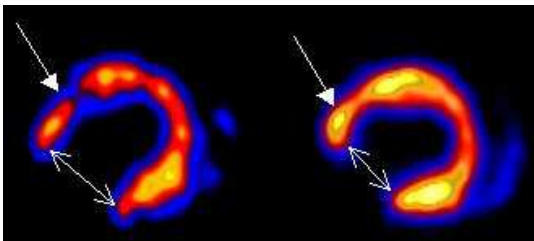


Figure 4.2 ^{18}F -FDG small animal PET axial images of an infarcted rat heart before and after regenerative therapy.



CONCLUSIONS

Small animal PET is safe for the serial assessment of laboratory animals, provides relevant data on tumour metabolism, on drug efficacy in animal models of human cancer and can be used in cardiology for the assessment of viable myocardium after infarction and/or regenerative therapy.